Effects of Variable Interstellar Environments on the Heliosphere

Hans-R. Müller[*,†], Gary P. Zank[†], Patrick Faurot-Pigeon[**], Vissuta Jiwariyavej[*], Rose Mutiso[*] and Fariha Shafi[*]

[*]*Department of Physics and Astronomy, Dartmouth College, Hanover NH 03755, USA*
[†]*Institute of Geophysics and Planetary Physics, University of California, Riverside CA 92521, USA*
[**]*Department of Mathematics, Columbia University, New York NY 10027, USA*

Abstract. A suite of global heliospheric models, for which the interstellar densities and temperatures are varied within reasonable bounds, is analyzed with respect to the heliospheric morphology and the locations of heliospheric boundaries, to arrive at empirical relations and to assess the sensitivity of the heliosphere to the interstellar conditions. Additionally, the differences between the termination shock at the Voyager 1 location and on the stagnation axis are discussed.

Keywords: local interstellar medium, heliosphere variability
PACS: 96.50.Ek, 96.50.Xy, 96.50.Zc

INTRODUCTION

The interaction of the local interstellar medium (LISM) with the solar wind gives rise to the global heliosphere. Interstellar plasma is excluded from entering the heliosphere and cannot be detected directly by spacecraft in the inner heliosphere. Interstellar neutral hydrogen (H) enters the heliosphere, and is being detected, but is processed on its way through the heliospheric regions because of its charge exchange interaction with the plasma protons. Hence, assessing the interstellar neutral densities with inner heliospheric measurements requires the use of complex, self-consistent neutral/plasma models and makes the interstellar proton and neutral H densities poorly constrained.

In order to make up for the lack of accurate knowledge of the interstellar densities, a grid of models is being computed by varying the interstellar densities and temperatures in a systematic way, within reasonable bounds. This establishes the sensitivity of certain key parameters of the heliosphere to the LISM boundary conditions, and thus can provide perspective for generalizing the results from the December 2004 termination shock crossing of Voyager 1.

A prior, less systematic parameter study in a very much larger region of LISM parameter space [Müller et al. 2006] assessed the reaction of the heliosphere to drastic changes in the interstellar environment. These changes come about when the Sun, on its path through the galaxy, encounters different ISM clouds and cloudlets. The global ISM differentiates itself into regions of different characteristic densities, velocities, and temperatures, and the Sun has been experiencing different conditions on time scales of tens of thousands to millions of years, while shorter time scale encounters are also possible. In contrast, the parameter study in this contribution adheres to LISM boundary conditions that could be called “contemporary”, as the Sun has been embedded in the

current moderately warm and dense ISM since at least 30,000 years.

PARAMETER STUDY CONTEXT

We are conducting a systematic study of the heliospheric reaction to different interstellar boundary parameters by calculating 64 multi-fluid heliospheric models. We test interstellar plasma densities $n_p = 0.05$, 0.11, 0.17, and 0.23 cm^{-3}, and interstellar neutral hydrogen densities $n_H = 0.05$, 0.11, 0.17, and 0.23 cm^{-3}. These densities bracket the weakly constrained proton and neutral hydrogen densities inferred from multiple observations [see, e.g., Zank 1999; Slavin and Frisch 2002]. From measurements of the interstellar neutral helium flow [Witte 2004; Möbius et al. 2004], the values of the interstellar velocity and temperature of $v = 26.3$ km s^{-1} and $T \sim 6300 \pm 340$ K are inferred. While we adopt the velocity value and keep it fixed for the entire parameter study, we test the interstellar temperature with four values, 4000, 6000, 8000, and 10,000 K. These values are meant to explore the effect of temperature variations on the heliosphere, and go well beyond the observed constraints. 80% of the 64 models have achieved preliminary convergence and form the subset from which we present preliminary results; the 12 models with $n_p = 0.23$ cm^{-3} and $n_H \geq 0.11$ cm^{-3} have not yet been modeled.

The interstellar medium boundary values are prescribed at a suitably large distance from the Sun (1000 AU). The solar wind enters the modeling region at an inner boundary of 1 AU. The solar wind is assumed to be independent of longitude, latitude, and time, with values of 5.0 cm^{-3} for the plasma density, a temperature of 10^5 K, and a radial velocity of 400 km s^{-1}. The models of the interaction of the solar wind with the ISM are carried out in a heliocentric frame of reference, and are effectively two-dimensional as we assume azimuthal symmetry about the stagnation axis (the axis parallel to the LISM flow that contains the Sun). To satisfy this assumption we also neglect heliospheric and interstellar magnetic fields.

To characterize the global heliospheres that result when the Sun is embedded in the different LISM environments as described above, we make use of the multi-fluid model developed by Zank et al. [1996]. The multi-fluid code simultaneously solves the time evolution of four interpenetrating fluids. One fluid represents the protons of the interstellar plasma component as well as the solar wind plasma. The remaining fluids model three thermodynamically distinct populations of neutral H. Each of the neutral fluids interacts with the plasma through resonant charge exchange, using the Fite et al. [1962] cross section, and all neutrals are subjected to photoionization. Radiation pressure is assumed to balance gravity. For a detailed description of the numerical model and the underlying physics, see Zank et al. [1996] and Zank [1999].

Modeling of heliospheric neutrals in the multi-fluid code as a superposition of three independent neutral fluids is an approximation to the general, non-Maxwellian neutral distribution function. Neutrals can also be calculated on a kinetic level without such an approximation [e.g., Baranov and Malama 1993; Müller et al. 2000]. Recent comparison studies [Alexashov and Izmodenov 2005; Heerikhuisen et al. 2006] have shown that the multi-fluid and kinetic methods are in essential agreement in most of the fine details concerning heliospheric geometry and shock locations, and even the distributions look similar. For this reason, we use the computationally less costly multi-fluid method here.

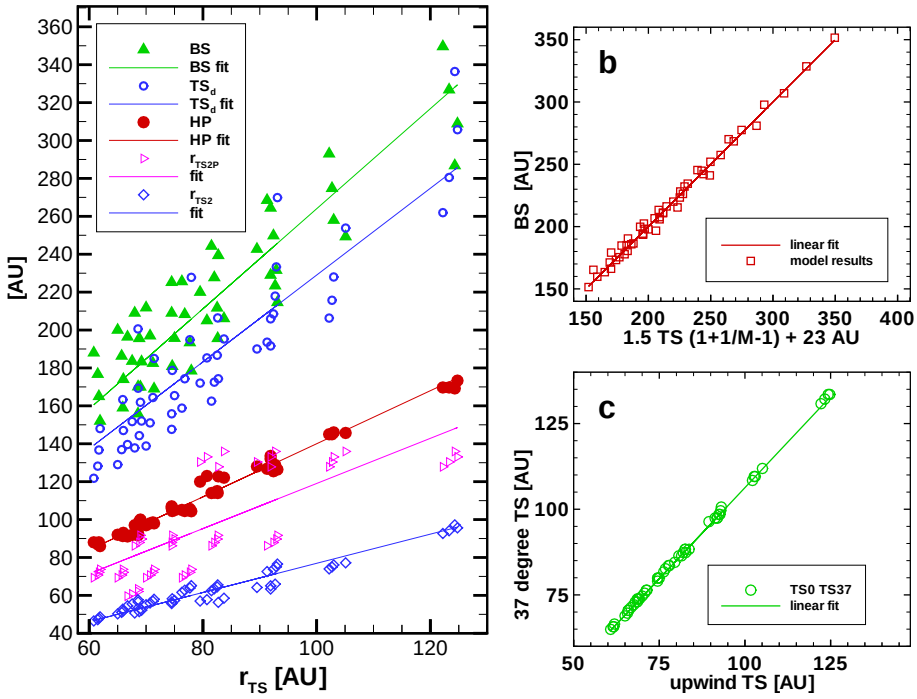


FIGURE 1. (a) Correlation between the upwind termination shock location r_{TS} and other distances, including the upwind heliopause HP (filled circles), the upwind bow shock (filled triangles), and the tailward TS distance (open circles), which are all model results. Also shown are the TS correlations with the distance r_{TS2} theoretically derived from plasma pressure balance (open triangles) and from total pressure balance (diamonds). Note the aspect ratio of 3:1 of the linear scales. (b) Correlation between the upwind bow shock location and the BS as predicted from r_{TS} and M via equation (5). (c) Correlation between TS locations in off-center and upwind direction.

PARAMETER STUDY RESULTS

The 52 models that result from the partial systematic parameter study outlined above represent heliospheres with a common morphology that includes a supersonic wind region bounded by a termination shock (TS), a heliosheath and a heliotail separated from the interstellar plasma at the heliopause (HP), and an interstellar bow shock (BS) decelerating the supersonic interstellar wind. The minimum TS distance is found at 60.8 AU in the upwind direction (defined as antiparallel to the LISM flow vector) for the highest density case at $T = 10^4$ K; the maximum distance is 336 AU in the downwind direction of the coldest and lowest density case. Upwind stagnation points (the nose of the HP) vary between 86 and 173 AU, and upwind BS distances from 152 to 350 AU.

The filled circles in Figure 1a display the upwind heliopause distance $r_{\rm HP}$ against the upwind TS distance $r_{\rm TS}$. Each filled circle is one particular model result, and the 52 results fit well to a linear relationship,

$$r_{\rm HP} = (1.40 \pm 0.03)\, r_{\rm TS}; \qquad (1)$$

the fit line is displayed in Figure 1a as well. Similarly, the correlation of the upwind

TS location with the downwind TS distance $r_{\rm TSd}$ is shown with open circles, and the correlation with the upwind bow shock $r_{\rm BS}$ as filled triangles.

It is clear from Figure 1a that while $r_{\rm TSd}$ and $r_{\rm BS}$ do correlate with $r_{\rm TS}$, the shown linear fits

$$r_{\rm BS} = (2.6 \pm 0.3)\, r_{\rm TS}, \quad r_{\rm TSd} = (2.3 \pm 0.3)\, r_{\rm TS}, \tag{2}$$

are quite poor. In fact, the data organize into clusters of four points with common n_p, n_H values, with the four probed interstellar temperatures creating the differences within a cluster. This behavior will be discussed further below.

The upwind TS distance is linked directly to the interstellar boundary parameters by

$$r_{\rm TS} = (1.30 \pm 0.08)\, r_{TS2} \tag{3}$$

where

$$\frac{r_{TS2}}{r_1} = \frac{16}{5} \frac{1}{\sqrt{3\sqrt{15}}} \sqrt{\frac{P_1}{P_{\rm tot}}} \left(1 - \frac{v^2}{v_{SW}^2}\right)^{\frac{5}{4}} \tag{4}$$

is the TS distance expected from the Rankine-Hugoniot shock transition conditions and treating the heliosheath and interstellar flows as incompressible [Suess and Nerney 1990; Zank 1999]. $P_1 = \rho_1 v_{SW}^2$ is the solar wind ram pressure, and ρ_1 the solar wind density, both taken at r_1 = 1 AU. v_{SW} and v are the solar wind and the interstellar speed, respectively, and $P_{\rm tot}$ is the total interstellar pressure; in particular for the 52 models, it is the ram pressure ρv^2 for the LISM with $\rho = m_p n_p + m_H n_H$. In Figure 1a, the calculated TS distances r_{TS2} are shown as open diamonds, and the linear fit (3) represents the data well. For comparison, the open triangles represent a similar relation for the assumption that only the plasma pressure (chiefly the plasma ram pressure) goes into $P_{\rm tot}$ in equation (4). The correlation is very poor in this case, which emphasizes the importance of the neutrals for the heliosphere (plasma and neutrals are not completely decoupled). If neutral H were tightly coupled to the plasma (i.e. if the mean free paths were very short compared to typical heliospherical length scales), then the factor in equation (3) should be one. However, the neutral-plasma coupling is neither zero nor very tight, such that the solar wind/LISM pressure balance for the heliospheres modeled here can only be described by the empirical factor of 1.3 in equation (3).

As mentioned above, the location of the BS does not only depend on the SW/LISM pressure balance, but also on the LISM temperature. This is illustrated in Figure 2 where the four models with $n_H = 0.17$ cm^{-3}, $n_p = 0.11$ cm^{-3} are displayed via their density and velocity profiles along the upwind stagnation axis. The overall pressure balance in these four models is essentially the same, and indeed, the HP locations (corresponding to the zeroes of $v(r)$) are almost identical. The BS locations vary much more widely, with the warmer models having a more distant BS. The hotter the LISM, the smaller the LISM Mach number (at infinity) and hence the weaker the bow shock, as seen in the less steep density and velocity gradients and the smaller post-shock density and velocity values that are attained. As adiabatic plasma deceleration needs to achieve $v = 0$ at a common distance, the standoff BS for larger LISM temperatures hence needs to occur farther out in the ISM. Assuming the simplest functional form for the correction of relation (2) with

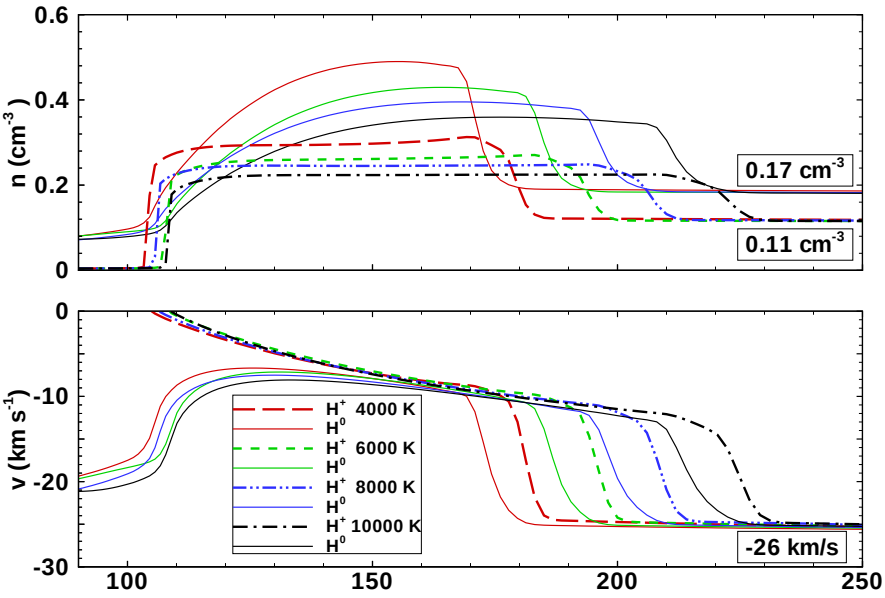


FIGURE 2. Density (top) and velocity (bottom) profiles of the four models with $n_H = 0.17$ cm^{-3}, $n_p = 0.11$ cm^{-3}, zooming in on the region between HP ($v = 0$; strong plasma density gradient) and the BS (n and v plasma gradients). Both plasma and neutral profiles are shown, the latter with solid lines.

approximately the right behavior at $M = 1$, an improved fit is

$$r_{\rm BS} = 1.5\, r_{TS} \left(1 + \frac{1}{M-1}\right) + 23{\rm AU}\,; \tag{5}$$

however, this is an empirical formula with no claim of validity outside $2 < M < 4$. The quality of the fit is illustrated in Figure 1b.

Figure 2 also contains the corresponding profiles for interstellar neutral H entering the heliosphere in the four illustrated cases. It can be seen that not far downstream of the bow shock, charge exchange leads to a reaction of the neutrals, with a slowdown and the formation of a hydrogen wall. A weak BS leads to less slowdown and hence to less overdensity at the peak of the hydrogen wall. However, the hydrogen wall is also "thicker" in that case, such that the amount of material, and in particular the amount of Ly-α absorption of stellar profiles by the hydrogen wall [e.g., Wood et al. 2000], remains largely independent of the LISM temperature.

The Voyager 1 (V1) crossing of the TS end of 2004 occurred at an ecliptic latitude of 35$^{\rm o}$ N, approximately 40$^{\rm o}$ away from the stagnation axis. With the TS being an aspherical surface (cf. eqn. 2), one has to expect the TS at V1 to be farther away than on the stagnation axis. The partial parameter study indicates that the distance in the direction of the V1 crossing is 6% farther out than the minimum ("nose") distance on the stagnation axis, and Figure 1c shows the corresponding data (for the closest available grid point at 37.5$^{\rm o}$), and a linear fit. The best fitting preliminary model for the V1 TS distance of 94 AU among the stationary models here has the parameters $n_H = 0.17$ cm^{-3}, $n_p = 0.05$ cm^{-3}, and $T = 8000$ K. Variations around these parameters in interstellar temperature result in TS shifts of at most 4 AU. Varying either plasma or

H density by 0.06 cm^{-3} results in shifts of 10–16 AU. Investigating other parameters at the V1 crossing site reveals (data not shown here) that for all other aspects, the global heliospheric models do not predict substantial differences between the TS at 37^o and the one on the stagnation axis. The compression ratio remains basically the same, and the neutral backgrounds are not distinguishable. It should be emphasized that these statements only apply to the axisymmetric, static models treated in this parameter study. A future consideration of the time dependent solar wind, as well as accounting for Voyager 1 probing the higher heliolatitude of the slow/fast solar wind transition, will modify these results towards a more realistic picture.

CONCLUSIONS

A systematic parameter study analyzing 52 self-consistent multi-fluid heliospheric models confirms basic ideas outlined by Müller et al. [2006] that the (static) size of the heliosphere is determined by the balance of solar wind and interstellar pressure, that the termination shock distance can be predicted by just knowing the LISM boundary conditions, and that the TS in the Voyager 1 direction, or the heliopause distance, then follow from empirical relations. The BS distance can be calculated as well; this requires taking additionally the LISM Mach number into account. The asymmetry of the TS (upwind/downwind ratio) is more involved and so far defies accurate capture. The neutral background at Voyager 1 is essentially the same as for the nose of the termination shock.

ACKNOWLEDGMENTS

This material is based upon work supported by NASA through the Astrophysics Theory Program under grant NAG5-13611, and through the Solar and Heliospheric Physics grant NAG5-12879, and by the Women in Science Program at Dartmouth College. GPZ and HRM acknowledge partial support from an NSF-DOE grant ATM-0296114 and NASA grants NAG5-12903 and NAG5-11621.

REFERENCES

1. D. Alexashov and V. V. Izmodenov, *Astron. Astrophys.* **439**, 1171 (2005).
2. V. Baranov and Y. Malama, *J. Geophys. Res.* **98**, 15157 (1993).
3. W. Fite, A. Smith, and R. Stebbings, *Proc. R. Soc. London Ser. A* **268**, 527 (1962).
4. J. Heerikhuisen, V. Florinski, and G. P. Zank, *J. Geophys. Res.* **111**, doi: 10.1029/2006JA011604, in press (2006).
5. E. Möbius et al., *Astron. Astrophys.* **426**, 897–907 (2004).
6. H.-R. Müller, G. P. Zank, and A. S. Lipatov, *J. Geophys. Res.* **105**, 27419–27438 (2000).
7. H.-R. Müller, P. C. Frisch, V. Florinski, and G. P. Zank, *Astrophys. J.* **647**, in press (2006).
8. J. D. Slavin and P. C. Frisch, *Astrophys. J.* **565**, 364–379 (2002).
9. S. T. Suess and S. Nerney, *J. Geophys. Res.* **95**, 6403–6412 (1990).
10. M. Witte, *Astron. Astrophys.* **426**, 835–844 (2004).
11. B. Wood, H.-R. Müller, and G. P. Zank, *Astrophys. J.* **542**, 493 (2000).
12. G. P. Zank, *Space Sci. Rev.* **89**, 413–688 (1999).
13. G. P. Zank, H. L. Pauls, L. L. Williams, and D. T. Hall, *J. Geophys. Res.* **101**, 21,639 (1996).